

Functional Characterization of a Partial Loss-of-Function Mutation of the Epithelial Sodium Channel (ENaC) Associated with Atypical Cystic Fibrosis

Regina Huber¹, Bettina Krueger¹, Alexei Diakov¹, Judit Korbmacher¹, Silke Haerteis¹, Jürgen Einsiedel², Peter Gmeiner², Abul Kalam Azad³, Harry Cuppens³, Jean-Jaques Cassiman³, Christoph Korbmacher¹ and Robert Rauh¹

¹Institut für Zelluläre und Molekulare Physiologie and ²Department Chemie und Pharmazie, Emil Fischer Centrum, Universität Erlangen-Nürnberg, ³Center of Human Genetics, KU Leuven

Key Words

Xenopus laevis oocytes • Electrophysiology • Heterologous expression • Ion channel

Abstract

Loss-of-function mutations of the epithelial sodium channel (ENaC) may contribute to pulmonary symptoms resembling those of patients with atypical cystic fibrosis (CF). Recently, we identified a loss-of-function mutation in the α -subunit of ENaC (α F61L) in an atypical CF patient without mutations in CFTR. To investigate the functional effect of this mutation, we expressed human wild-type $\alpha\beta\gamma$ -ENaC or mutant $\alpha_{F61L}\beta\gamma$ -ENaC in *Xenopus laevis* oocytes. The α F61L mutation reduced the ENaC mediated whole-cell currents by ~90%. In contrast, the mutation decreased channel surface expression only by ~40% and did not alter the single-channel conductance. These findings indicate that the major effect of the mutation is a reduction of the average channel open probability (P_o). This was confirmed by experiments using the β S520C mutant ENaC which can be converted to a channel with a P_o of nearly one, and by experiments

using chymotrypsin to proteolytically activate the channel. These experiments revealed that the mutation reduced the average P_o of ENaC by ~75%. Na^+ self inhibition of the mutant channel was significantly enhanced, but the observed effect was too small to account for the large reduction in average channel P_o . The ENaC-activator S3969 partially rescued the loss-of-function phenotype of the α F61L mutation. We conclude that the α F61L mutation may contribute to respiratory symptoms in atypical CF patients.

Copyright © 2010 S. Karger AG, Basel

Introduction

The amiloride-sensitive epithelial sodium channel (ENaC) is a member of the ENaC/degenerin family of non-voltage gated ion channels. It is localized in the apical membrane of sodium absorbing epithelial cells, e.g. in the respiratory tract, in distal nephron, distal colon, sweat and salivary ducts. In these epithelia ENaC is the

rate limiting step for sodium absorption [1, 2]. In the lung fluid absorption critically depends on ENaC function [3]. ENaC is believed to form a heterotrimeric channel composed of three homologous subunits α , β and γ [4-6]. Each subunit has two transmembrane domains, a large extracellular loop and cytosolic N- and C-termini [1].

Cystic fibrosis (CF) is an autosomal recessive hereditary disease which affects different organs like lung, intestine, pancreas, reproductive organs and sweat glands. It is usually caused by a mutation in the cystic fibrosis transmembrane conductance regulator (CFTR) gene, which encodes a Cl^- channel localized in the apical membrane of a wide range of epithelial cells. Thus, CF epithelia have a reduced apical Cl^- conductance. The clinical phenotype of the patients is very heterogeneous including chronic sinopulmonary disease, gastrointestinal or nutritional symptoms (e.g. exocrine pancreatic insufficiency, failure to thrive), salt loss syndromes, or congenital bilateral absence of the vas deferens [7]. Patients with so-called classical or typical CF show at least one phenotypic characteristic and a sweat chloride concentration >60 mmol/l. In non-classic or atypical CF at least one phenotypic characteristic is combined with a normal (<30 mmol/l) or borderline (30-60 mmol/l) sweat chloride concentration. Most of the patients with atypical CF have relatively mild symptoms. However, the CF phenotype is a continuum of symptoms and cannot be easily defined in two distinct disease categories (typical versus atypical CF), although the tentative diagnosis of atypical CF is clinically helpful [7]. The large variability of CF symptoms suggests that CF modifier genes exist. Interestingly, the genes encoding the β - and γ -subunits of ENaC have recently been reported to be potential modifier genes in CF [8]. Moreover, the TNF α receptor located next to the gene encoding the α -subunit of ENaC has been identified as a potential modifier gene [8].

A functional interaction of ENaC and CFTR is suspected to play an important role in the pulmonary pathophysiology of CF [9]. A fine tuned balance between Cl^- secretion *via* CFTR and Na^+ absorption *via* ENaC determines the height and the viscosity of the so-called airway surface liquid (ASL) layer, which is an important factor for mucus clearance of the lungs [9]. Defective CFTR results in enhanced Na^+ absorption which leads to sticky mucus and impairs mucociliary clearance which is a fundamental defect in CF airways. However, CFTR deficient mice (CFTR $-/-$) do not develop severe pulmonary symptoms typical for human CF [10, 11]. In contrast, transgenic mice specifically overexpressing the ENaC β -subunit in the airways develop a CF-like

pulmonary phenotype [12]. This is probably caused by enhanced Na^+ and fluid absorption resulting in reduced mucociliary clearance. Interestingly, preventive amiloride therapy reduces morbidity and mortality of lung disease in these β ENaC over-expressing mice [13]. These findings suggest that ENaC gain-of-function mutations may contribute to CF pathophysiology.

Loss-of-function mutations of ENaC were identified in patients suffering from pseudohypoaldosteronism type 1 (PHA1), a rare congenital disease characterized by renal salt-wasting, hyperkalemia, metabolic acidosis, dehydration and low arterial blood pressure [14]. Interestingly, some PHA1 patients also suffer from CF-like pulmonary symptoms [15-17]. Moreover, in atypical CF-patients with pulmonary symptoms but without mutations in CFTR, Sheridan et al. [18] identified loss-of-function mutations in the extracellular loop of the β -subunit of ENaC. The pathophysiological mechanism by which reduced ENaC function may cause pulmonary symptoms is not yet clear. However, it is tempting to speculate that a reduced Na^+ absorption on the basis of a reduced ENaC activity occurs in combination with an enhanced Cl^- secretion *via* CFTR, thereby increasing the height of the ASL. Indeed, in a small number of PHA1 patients an increased ASL and an enhanced mucociliary clearance have been demonstrated [19].

From the findings discussed above it has been proposed that gain-of-function as well as loss-of-function mutations of ENaC may contribute to pulmonary symptoms that result in the clinical diagnosis of atypical CF [18, 20]. Indeed, we recently identified several ENaC mutations in patients with CF-like disease in whom a mutation could not be identified on both CFTR genes. Interestingly, these included gain-of-function and loss-of-function mutations. One of the newly identified loss-of-function mutations from a patient with CF-like lung symptoms and a positive sweat test is localized in the α -subunit of ENaC (α F61L) [21]. The aim of the present study was to characterize the effects of this α F61L mutation on ENaC function and to investigate the mechanisms underlying the partial loss-of-function phenotype of the mutant channel.

Materials and Methods

Plasmids

Full length cDNAs for all human ENaC subunits were cloned in pcDNA3.1. Linearized plasmids were used as templates for cRNA synthesis using T7 RNA polymerases (mMessage mMachine, Ambion, Austin, TX). To minimize the

risk of expression artifacts that may arise from differences in cRNA quality, cRNAs for wild-type and mutant ENaC were synthesized in parallel and the experiments were performed using at least two different batches of cRNA. The β S520C mutant was generated by site-directed mutagenesis (QuikChange® Site-Directed Mutagenesis Kit, Stratagene, Amsterdam, Netherlands). A FLAG reporter epitope was inserted in the extracellular loop of the β -subunit with site-directed mutagenesis extension overlap PCR at the corresponding site as previously described for rat β ENaC [22]. Mutations were confirmed by sequence analysis.

Isolation of Oocytes and Injection of cRNA

Oocytes were obtained from adult female *Xenopus laevis* in accordance with the principles of German legislation, with approval by the animal welfare officer for the University of Erlangen-Nürnberg, and under the governance of the state veterinary health inspectorate. Animals were anaesthetized in 0.2% MS222 (Sigma, Taufkirchen, Germany). Ovarian lobes were obtained by partial ovariectomy and oocytes were isolated by enzymatic digestion at 19°C for 3-4 hours with 600-700 U/ml type 2 collagenase from *Cl. histolyticum* (CLS 2, Worthington, Lakewood, NJ) dissolved in OR2 solution containing (in mM) NaCl 82.5, KCl 2, MgCl₂ 1, and HEPES 1 (pH 7.4 with Tris). Defolliculated stage V-VI oocytes were injected (Nanject II automatic injector, Drummond, Broomall, PA) with 0.5 ng or 1 ng cRNA per subunit of ENaC. The cRNAs were dissolved in RNase-free water and the total volume injected was 46 nl. Injected oocytes were stored at 19°C in a solution containing (in mM) NMDG (N-methyl-D-glucamine)-Cl 87, NaCl 9, KCl 2, CaCl₂ 1.8, MgCl₂ 1, and HEPES 5 (pH 7.4 with Tris) supplemented with 100 units/ml penicillin and 100 µg/ml streptomycin to prevent bacterial overgrowth.

Two-Electrode Voltage-Clamp

Oocytes were routinely studied 1-2 days after injection using the two-electrode voltage-clamp technique (TEVC) as described previously [23, 24]. The oocytes were placed in a small experimental chamber and constantly superfused at room temperature with ND96 (in mM: NaCl 96, KCl 2, CaCl₂ 1.8, MgCl₂ 1, HEPES 5, pH 7.4 with Tris) supplemented with amiloride (2 µM, Sigma) at a rate of 2-3 ml/min. Bath solution exchanges were controlled by a magnetic valve system (ALA BPS-8) in combination with a TIB14 interface (HEKA, Lambrecht, Germany). Voltage-clamp experiments were performed using an OC-725C amplifier (Warner Instruments Corp., Hamden, CT) interfaced via a LIH-1600 (HEKA) to a PC running PULSE 8.67 software (HEKA) for data acquisition and analysis. For continuous whole-cell current recordings oocytes were routinely clamped at a holding potential of -60 mV. Amiloride-sensitive whole-cell currents (ΔI_{ami}) were determined by washing out amiloride with amiloride-free ND96 and subtracting the whole-cell currents measured in the presence of amiloride from the corresponding whole-cell currents recorded in the absence of amiloride. Downward current deflections in the current traces correspond to inward currents, i.e. movement of positive charge from the extracellular side into the cell. For the detection of Na⁺ self inhibitor oocytes were continuously clamped at -100 mV

and superfused at a rate of 8-10 ml/min, initially with a 1 mM Na⁺ solution (in mM: NMDG-Cl 109, NaCl 1, KCl 2, CaCl₂ 1.8, MgCl₂ 1, HEPES 5, pH 7.4 with Tris) followed by a rapid change to a 110 mM Na⁺ solution (in mM: NaCl 110, KCl 2, CaCl₂ 1.8, MgCl₂ 1, HEPES 5, pH 7.4 with Tris).

Patch-clamp

Single-channel recordings in conventional outside-out patches were essentially performed as described previously using oocytes kept in low sodium modified Barth's saline after cRNA injection to prevent Na⁺ overloading [25, 26]. Pipettes were filled with K-gluconate pipette solution (in mM: K-gluconate 90, NaCl 5, Mg-ATP 2, EGTA 2, and HEPES 10 adjusted to pH 7.28 with Tris). Seals were routinely formed in a NMDG-Cl bath solution (in mM: NMDG-Cl 95, NaCl 1, KCl 4, MgCl₂ 1, CaCl₂ 1, HEPES 10, pH 7.4 with Tris). In NaCl bath solution the NMDG-Cl was replaced by 95 mM NaCl. Downward current deflections correspond to cell membrane inward currents, i.e. movement of positive charge from the extracellular side to the cytoplasmic side. Outside-out patches were routinely held at a holding pipette potential of -70 mV which was close to the calculated reversal potential of Cl⁻ ($E_{Cl} = -77.2$ mV) and K⁺ ($E_K = -79.4$ mV) under our experimental conditions with experiments performed at room temperature. Single-channel current data were filtered at 10 kHz with a 3-pole Bessel filter and at 500 Hz with a 4-pole Bessel filter and sampled at 2 kHz. Single-channel current traces were re-filtered at 50 Hz to estimate the single-channel current amplitude derived from binned amplitude histograms [25-27].

Surface Labelling

ENaC surface expression was determined with a chemiluminescence assay essentially as described previously [23, 24, 28, 29]. All incubation steps were performed on ice and no glassware was used. Unspecific binding sites were blocked by 30 min incubation in ND96 supplemented with 1% bovine serum albumine (BSA, Sigma). Subsequently oocytes were incubated for 1 h in primary mouse anti-FLAG M2 monoclonal antibody (1 µg/ml, Sigma, Taufkirchen, Germany), washed 6x3 min in ND96+BSA, incubated for 45 min in secondary peroxidase-conjugated sheep anti-mouse IgG (1 µg/ml, Chemicon, Boronia Victoria, Australia), washed 6x3 min in ND96+BSA and finally 6x3 min in ND96. Individual oocytes were placed in a white U-bottom 96 well plate and 50 µl of SuperSignal ELISA FEMTO Maximum Sensitivity Substrate (Pierce, Rockford, IL) were added to each oocyte. Chemiluminescence was quantified with a Tecan GENios microplate reader (TECAN, Crailsheim, Germany). Results are given in relative light units (RLU).

Chemicals

S3969 was synthesized essentially as described previously [30]. ¹H-NMR and mass spectra were carefully compared with those kindly provided by Brian D. Moyer (San Diego, CA) to confirm identity of the synthesized substance. MTSET (2-(trimethylammonium)ethyl methanethiosulphonate bromide) was obtained from Toronto Research Chemicals (Toronto, Canada), α -chymotrypsin from bovine pancreas, type II, and amiloride were from Sigma (Taufkirchen, Germany).

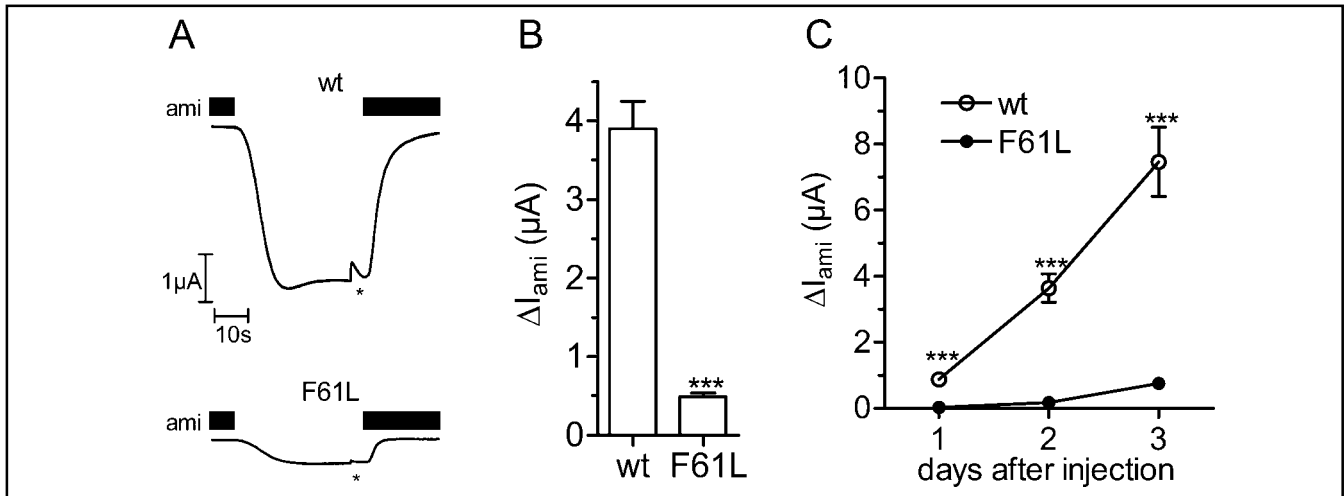


Fig. 1. α F61L mutation decreases ENaC mediated Na^+ currents in *Xenopus laevis* oocytes. Oocytes were injected with cRNAs coding for $\alpha\beta\gamma$ -ENaC (wt) or $\alpha_{F61L}\beta\gamma$ -ENaC (F61L). Amiloride-sensitive whole-cell currents (ΔI_{ami}) were measured using the two-electrode voltage-clamp technique. **A:** Representative whole-cell current traces of an oocyte expressing $\alpha\beta\gamma$ -ENaC (upper trace) or $\alpha_{F61L}\beta\gamma$ -ENaC (lower trace). Amiloride (ami, 2 μ M) was present in the bath solution during the time periods indicated by black bars. At the times indicated by asterisks voltage pulse current responses were removed from the traces for clarity. **B:** Summary of similar experiments as shown in **A** performed in three different batches of oocytes with $n=45$ in each experimental group. **C:** ΔI_{ami} of $\alpha\beta\gamma$ - and $\alpha_{F61L}\beta\gamma$ -ENaC expressing oocytes detected one, two, and three days after cRNA injection. Each data point represents the mean ΔI_{ami} measured in 11 to 13 individual oocytes. SEM values are represented by vertical bars unless they are smaller than the symbols used. *** $p<0.001$

Statistical Methods

Data are presented as mean \pm SEM. N indicates the number of different batches of oocytes, n the number of individual oocytes studied. Statistical significance was assessed by appropriate version of Student's t-test using GraphPad Prism 4.03 for Windows (GraphPad Software, Inc., San Diego, CA). To quantify Na^+ self inhibition we used the model described by Chraïbi & Horisberger [31] in which the current I_t is given as a function of time by

$$I_t = I_{max} \frac{k_a + k_i e^{-t(k_a + k_i)}}{k_a + k_i} (1 - k_{down} t) \quad (1)$$

with the activation rate constant k_a , the inactivation rate constant k_i , the rundown rate constant k_{down} , and the maximum current at $t=0$ I_{max} . Rate constants were determined with equation (1) and the nonlinear regression/curve fit function method of Prism 4.03, starting from the inflection point of the current declining phase of each trace [31]. I_{max} was determined by extrapolation to $t=0$.

Results

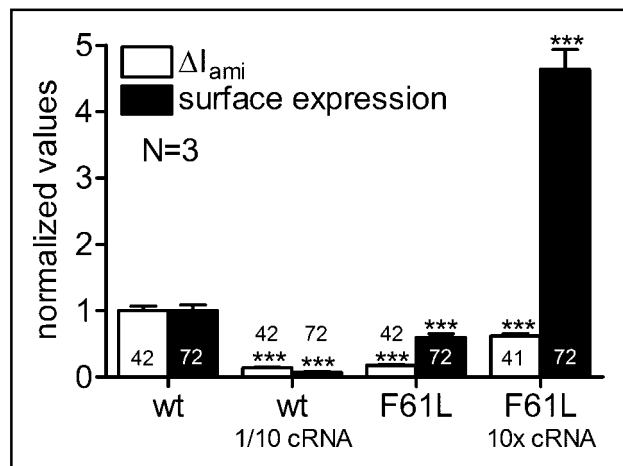
*α F61L inhibits ENaC mediated whole-cell currents in *Xenopus laevis* oocytes*

To investigate the effect of the α F61L mutation on ENaC function, we expressed wild-type $\alpha\beta\gamma$ -ENaC and mutant $\alpha_{F61L}\beta\gamma$ -ENaC in *Xenopus laevis* oocytes.

The two-electrode voltage-clamp technique was used to determine ENaC mediated whole-cell currents. Fig. 1A shows representative whole-cell current traces from an oocyte expressing $\alpha\beta\gamma$ -ENaC (upper trace) or $\alpha_{F61L}\beta\gamma$ -ENaC (lower trace). Oocytes were clamped at a holding potential of -60 mV, and the recordings were started in the presence of amiloride (2 μ M) to specifically inhibit ENaC. Washout of amiloride revealed a sizeable inward current component which represents the ENaC mediated Na^+ inward current. Re-addition of amiloride returned the whole-cell current toward the initial baseline level. As illustrated by these traces, the amiloride-sensitive whole-cell current (ΔI_{ami}) was much smaller in oocytes expressing the mutant channel than in control oocytes expressing wild-type ENaC. In three different batches of oocytes ΔI_{ami} averaged 3.9 ± 0.35 μA in $\alpha\beta\gamma$ -ENaC expressing control oocytes ($n=45$) and 0.5 ± 0.05 μA in $\alpha_{F61L}\beta\gamma$ -ENaC expressing oocytes ($n=45$, $p<0.001$) (Fig. 1B). Thus, the α F61L mutation reduced the ENaC mediated sodium whole-cell current by about 90%.

In addition, in one batch of oocytes we also measured ΔI_{ami} over three days after cRNA injection (Fig. 1C). As shown in Fig. 1C in wild-type and mutant ENaC expressing oocytes ΔI_{ami} increased from day one to day three, which probably reflects the fact that with longer incubation periods more time is available for ENaC

Fig. 2. Channel surface expression is reduced in $\alpha_{F61L}\beta\gamma$ -ENaC expressing oocytes. Channel surface expression was detected by insertion of a FLAG reporter epitope in the extracellular loop of the β -subunit and quantified by a chemiluminescence assay. Surface expression (black columns) and ΔI_{ami} (open columns) were obtained in parallel in $\alpha\beta_{FLAG}\gamma$ -ENaC (wt) and $\alpha_{F61L}\beta_{FLAG}\gamma$ -ENaC (F61L) expressing oocytes. Oocytes injected with 1/10 amount of cRNA for $\alpha\beta_{FLAG}\gamma$ -ENaC or the 10-fold amount of cRNA for $\alpha_{F61L}\beta_{FLAG}\gamma$ -ENaC served as controls. To pool data from different batches of oocytes, individual current and surface expression values were normalized to the corresponding mean values of $\alpha\beta_{FLAG}\gamma$ -ENaC expressing control oocytes. Numbers inside or above the columns indicate the number of individual oocytes measured. N indicates number of different batches of oocytes. *** $p < 0.001$



synthesis and channel delivery to the plasma membrane [32]. Importantly, on all days ΔI_{ami} was significantly lower in mutant ENaC expressing oocytes than in wild-type ENaC expressing oocytes. This confirms that the inhibitory effect of the α F61L mutation on ENaC currents is a robust phenomenon. With Western blot analysis we detected similar expression levels of wild-type and mutant channel protein (data not shown). This suggests that the inhibitory effect of the α F61L mutation is based on impaired ENaC function rather than on defective protein expression.

Surface expression of $\alpha_{F61L}\beta\gamma$ -ENaC is decreased

The ENaC mediated whole-cell current results from the sum of the Na^+ currents through individual active channels, i.e. the product of the number of channels expressed at the plasma membrane, the single-channel current amplitude, and the channel open probability (P_o). The inhibitory effect of the α F61L mutation may be caused by an individual or combined decrease of these factors. Therefore, we assessed channel surface expression by using a FLAG-tagged β -subunit of ENaC (β_{FLAG}) and a chemiluminescence assay. In three different batches of oocytes ENaC surface expression was ~40% lower in $\alpha_{F61L}\beta_{FLAG}\gamma$ -ENaC expressing oocytes (n=72) compared to $\alpha\beta_{FLAG}\gamma$ -ENaC expressing oocytes (n=72, $p < 0.001$) (Fig. 2). In matched oocytes the inhibitory effect of the mutated α -subunit on ΔI_{ami} was much larger than the observed reduction in channel surface expression. Thus, a decrease in channel surface expression cannot fully explain the large inhibitory effect of the mutation on ENaC currents. To confirm that the chemiluminescence assay can reliably detect a decrease in channel surface expression under our experimental conditions, we performed control experiments in which the amount of cRNA for $\alpha\beta_{FLAG}\gamma$ -ENaC injected per oocyte was

reduced to one tenth of the usual amount. As expected, this largely reduced both, ENaC currents and surface expression. As an additional control the amount of cRNA for $\alpha_{F61L}\beta_{FLAG}\gamma$ -ENaC injected per oocyte was increased by 10-fold. This resulted in the expected increase of both, channel surface expression and ΔI_{ami} (Fig. 2). Non injected control oocytes showed negligible luminescence activity and no measurable ΔI_{ami} (data not shown). Our findings indicate that the surface expression assay works reliably and that the mutation has a more dramatic effect on ENaC currents than on ENaC surface expression. The slightly reduced surface expression is likely to contribute to the partial loss-of-function phenotype of the mutant channel but cannot explain the large inhibitory effect of the mutation on ENaC whole-cell currents.

Single-channel current is not reduced in $\alpha_{F61L}\beta\gamma$ -ENaC

In principle, a reduction of the single-channel current amplitude could contribute to the inhibitory effect of the α F61L mutation. Therefore, we assessed single-channel current amplitudes in outside-out patches of oocytes expressing $\alpha\beta\gamma$ -ENaC or $\alpha_{F61L}\beta\gamma$ -ENaC. Fig. 3A shows single-channel current traces of wild-type (left) and mutant ENaC (right) at different holding potentials. Fig. 3B summarizes data from similar recordings. There was no significant difference in the single-channel current amplitude between wild-type and mutant ENaC at a holding potential of -40 mV (wt: -0.25 ± 0.005 pA, n=9, F61L: -0.27 ± 0.006 pA, n=4, $p = 0.109$) and -70 mV (wt: -0.37 ± 0.005 pA, n=14, F61L: -0.38 ± 0.004 pA, n=5, $p = 0.118$). Using these data we can estimate a single-channel conductance of about 5 pS for both, the wild-type and the mutant channel, which is in good

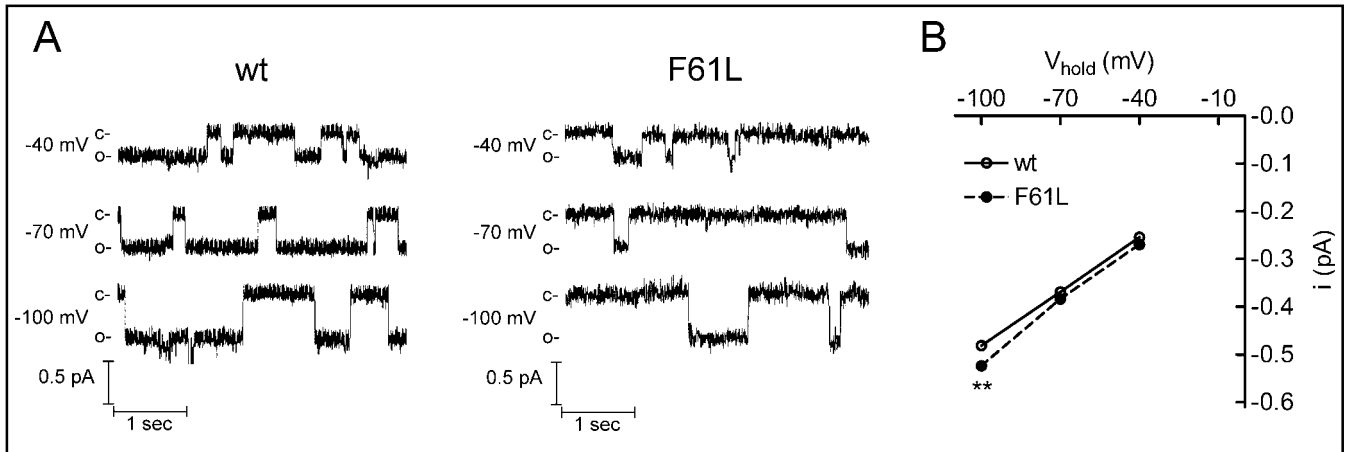


Fig. 3. Single-channel conductance is not reduced in α F61L mutant ENaC. A: Patch-clamp recordings of an $\alpha\beta\gamma$ -ENaC (wt) and an $\alpha_{F61L}\beta\gamma$ -ENaC (F61L) containing outside-out patch at different holding potentials (-40 mV, -70 mV, -100 mV). Please note that the single-channel P_o of the mutant channel appeared to be lower (~ 0.2) than that of the wild-type channel (~ 0.6). Open and closed levels are indicated by o- and c-, respectively. B: Average single-channel IV-plots from similar outside-out patch clamp recordings as shown in A. Error bars are hidden by the symbols. ** $p < 0.01$

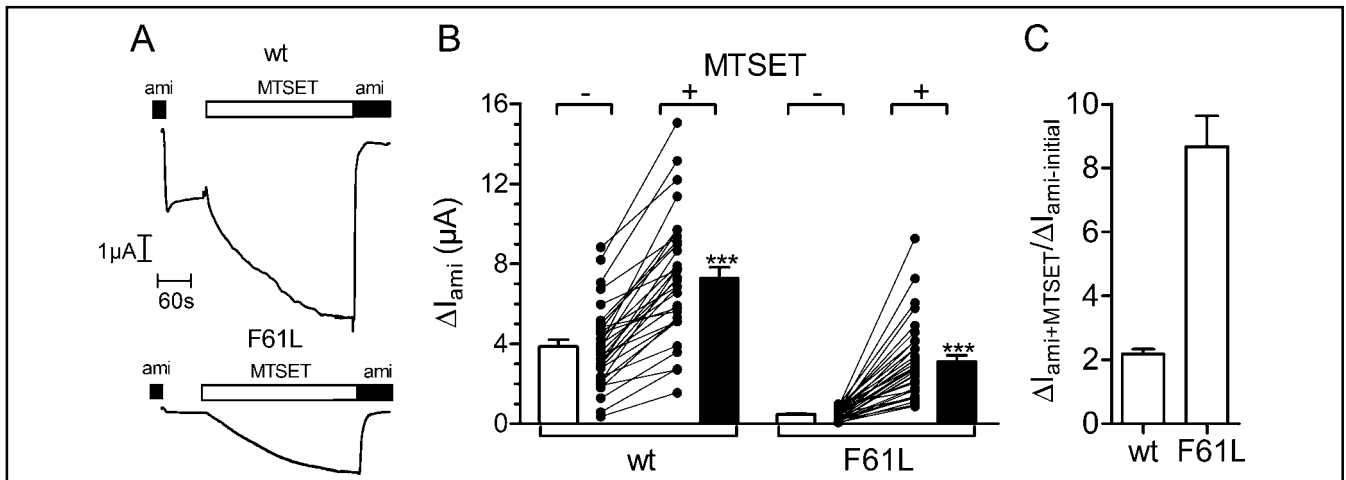


Fig. 4. Average open probability (P_o) of ENaC is reduced in oocytes expressing the α F61L mutant channel. A: Representative whole-cell current traces of an $\alpha\beta_{S520C}\gamma$ -ENaC (wt, upper trace) and an $\alpha_{F61L}\beta_{S520C}\gamma$ -ENaC (F61L, lower trace) expressing oocyte. The β_{S520C} -mutation makes ENaC sensitive to MTSET (1 mM) which can increase the average P_o of channels containing this mutant β -subunit to nearly one. This increase in P_o upon application of MTSET is reflected by the activation of an inward current component in the whole-cell current traces shown. B: Summary of similar experiments as shown in A performed in oocytes from 3 different batches with $n=31$ (wt) or $n=34$ (F61L). C: Same data as shown in B but normalized to the corresponding control value before MTSET application to demonstrate the relative stimulatory effect of MTSET on ΔI_{ami} . *** $p < 0.001$

agreement with previously reported data for human ENaC [33]. At -100 mV the single-channel current amplitude of mutant ENaC (-0.52 ± 0.005 pA, $n=5$) was marginally higher than that of wild-type ENaC (-0.48 ± 0.007 pA, $n=14$, $p=0.003$). Thus, we conclude that the mutation has no major effect on the single-channel sodium conductance of ENaC and that a reduced single-channel conductance

does not contribute to the inhibitory effect of the α F61L mutation.

Average channel open probability (P_o) is reduced in $\alpha_{F61L}\beta\gamma$ -ENaC

Since the observed 40% decrease in surface expression cannot fully explain the large inhibitory effect of the

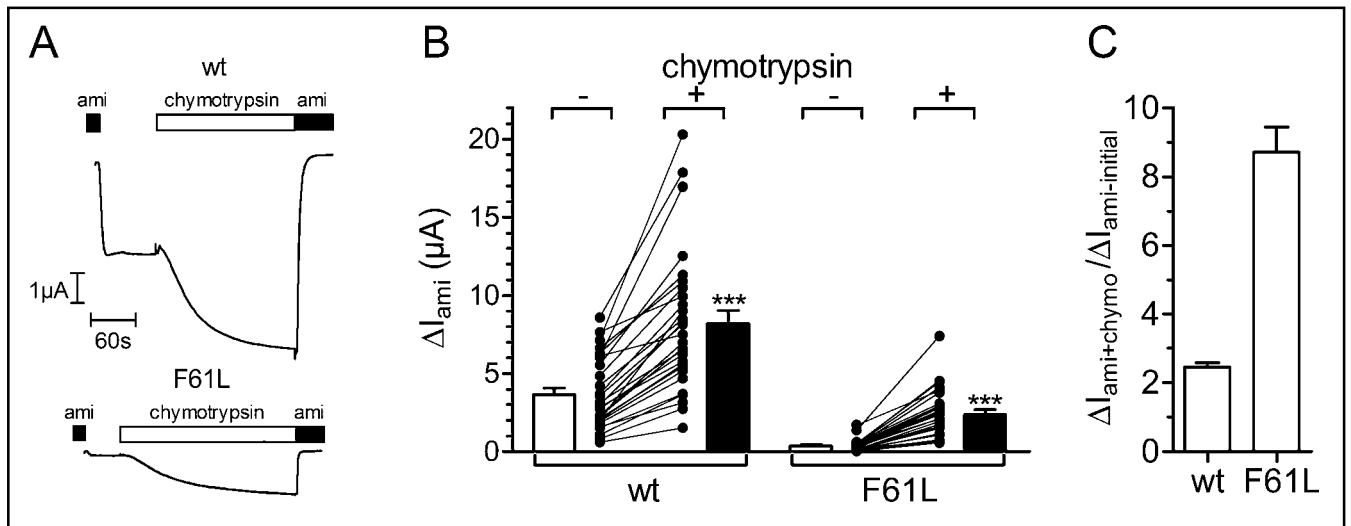


Fig. 5. The stimulatory effect of chymotrypsin on the α F61L mutant ENaC is enhanced. A: Representative whole-cell current traces of an $\alpha\beta\gamma$ -ENaC (wt, upper trace) and an $\alpha_{F61L}\beta\gamma$ -ENaC (F61L, lower trace) expressing oocyte. Chymotrypsin (2 μ g/ml) was applied to proteolytically activate ENaC. B: Summary of similar experiments as shown in A performed in oocytes from 3 different batches with $n=28$ for each experimental group. C: Same data as shown in B but normalized to the corresponding control value before chymotrypsin application to demonstrate the relative stimulatory effect of chymotrypsin on ΔI_{ami} . *** $p<0.001$

α F61L mutation on ENaC whole-cell currents, we hypothesized that the mutation mainly reduces the average P_o of ENaC. Our single-channel recordings (Fig. 3A) support but do not prove this hypothesis, because longer recordings with only one active channel in the patch would be needed for reliable P_o measurements. Moreover, it is well known that ENaC displays a wide range of rather variable P_o values (from <0.1 to 0.9) when studied at the single-channel level [1, 2]. Thus, it is inherently difficult to estimate an average P_o for ENaC from single-channel recordings. Therefore, to further investigate this issue, we used the S520C mutant of β ENaC (β S520C). A channel with this mutant subunit is thought to be converted to a channel with a P_o of nearly one by exposure to the positively charged sulfhydryl reagent MTSET, which destabilizes the closed state of the channel [30, 34, 35]. As illustrated by two representative whole-cell current traces in Fig. 4A, application of MTSET caused a substantial increase in ΔI_{ami} in both, $\alpha\beta_{S520C}\gamma$ -ENaC and $\alpha_{F61L}\beta_{S520C}\gamma$ -ENaC expressing oocytes. However, the relative stimulatory effect was much bigger in oocytes expressing the α F61L mutation. Results from similar experiments are summarized in Fig. 4B and confirm that the baseline ENaC currents measured before the application of MTSET were smaller in $\alpha_{F61L}\beta_{S520C}\gamma$ -ENaC than in $\alpha\beta_{S520C}\gamma$ -ENaC expressing oocytes. Interestingly, after exposure to MTSET ΔI_{ami} values were still lower in mutant ENaC expressing oocytes than in control oocytes.

Under the assumption that both, wild-type ENaC and mutant ENaC, have the same single-channel conductance and reach a similar P_o after treatment with MTSET, this would mean that fewer mutant than wild-type channels are expressed at the plasma membrane. This conclusion is consistent with our surface expression data (see above). On average, MTSET increased ΔI_{ami} 2.2-fold in control oocytes and 8.7-fold in oocytes expressing the α F61L mutant (Fig. 4C). If MTSET converted the open probability of all active ion channels present at the cell surface to one, these findings indicate that the average P_o of the channels prior to the application of MTSET must have been higher in $\alpha\beta_{S520C}\gamma$ -ENaC expressing oocytes than in $\alpha_{F61L}\beta_{S520C}\gamma$ -ENaC expressing oocytes.

Chymotrypsin activates $\alpha_{F61L}\beta\gamma$ -ENaC more than $\alpha\beta\gamma$ -ENaC

ENaC can be activated by extracellular proteases like trypsin, chymotrypsin, and neutrophil elastase [25, 36-39]. Since the α F61L mutation largely reduces average channel P_o , we wondered whether the mutation alters the responsiveness of the channel to extracellular proteases. As a prototypical protease we used chymotrypsin which has a robust stimulatory effect on ENaC and, unlike trypsin, does not cause a transient stimulation of a calcium-activated chloride conductance in the oocyte expression system [25, 36, 40]. Fig. 5A shows two representative whole-cell current traces from an oocyte

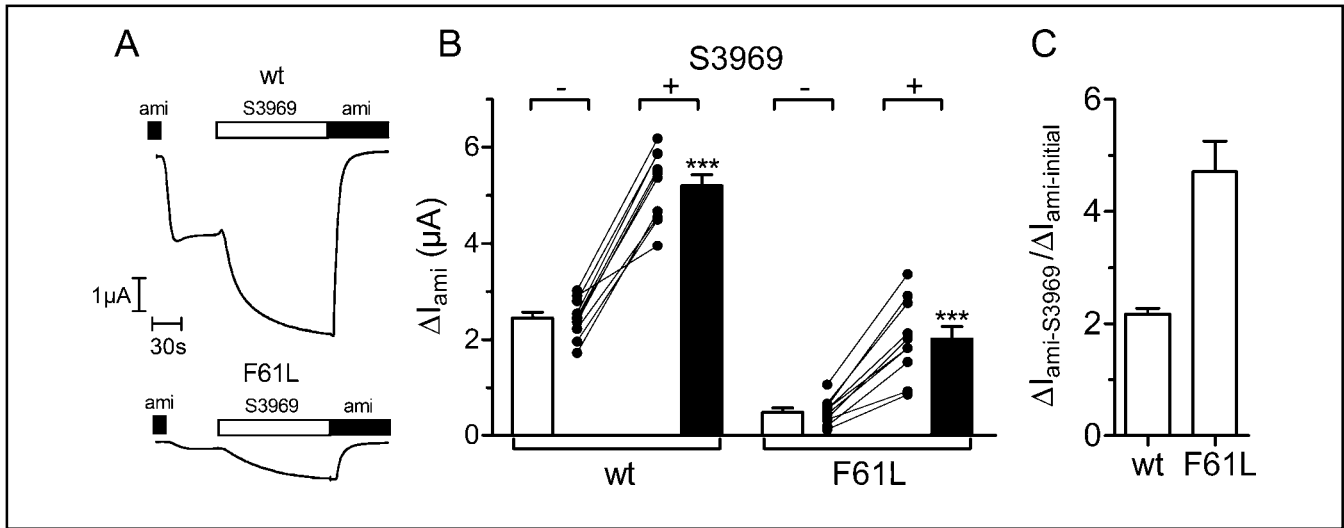


Fig. 6. The novel ENaC-activator S3969 stimulates α F61L mutant ENaC more than wild-type ENaC. A: Representative traces of an $\alpha\beta\gamma$ -ENaC (wt, upper trace) and an $\alpha_{F61L}\beta\gamma$ -ENaC (F61L, lower trace) expressing oocyte. S3969 (10 μ M) was applied to activate ENaC. B: Summary of similar experiments as shown in A performed in n=10 oocytes for each experimental group. C: Same data as shown in B but normalized to the corresponding control value before S3969 application to demonstrate the relative stimulatory effect of S3969 on ΔI_{ami} . *** p<0.001

expressing $\alpha\beta\gamma$ -ENaC (left) or $\alpha_{F61L}\beta\gamma$ -ENaC (right). Application of chymotrypsin (2 μ g/ml) activated inward currents in both, $\alpha\beta\gamma$ -ENaC and $\alpha_{F61L}\beta\gamma$ -ENaC expressing oocytes. Results from similar experiments are summarized in Fig. 5B and confirm that the baseline ENaC currents measured before the application of chymotrypsin were smaller in $\alpha_{F61L}\beta\gamma$ -ENaC than in $\alpha\beta\gamma$ -ENaC expressing oocytes. On average, chymotrypsin increased ΔI_{ami} 2.4-fold in control oocytes and 8.2-fold in oocytes expressing $\alpha_{F61L}\beta\gamma$ -ENaC (Fig. 5C). Thus, the relative stimulatory effect of chymotrypsin on the mutant channel is much larger than that on wild-type ENaC. Proteolytic channel activation is expected to have a more pronounced effect on channels with a low baseline P_o than on channels with a P_o that is already high before channel activation by an extracellular protease [25]. Therefore, the results of our chymotrypsin experiments are consistent with our conclusion from the MTSET experiments that the average baseline channel P_o of the mutant channel is reduced.

The novel ENaC-activator S3969 stimulates $\alpha_{F61L}\beta\gamma$ -ENaC more than $\alpha\beta\gamma$ -ENaC

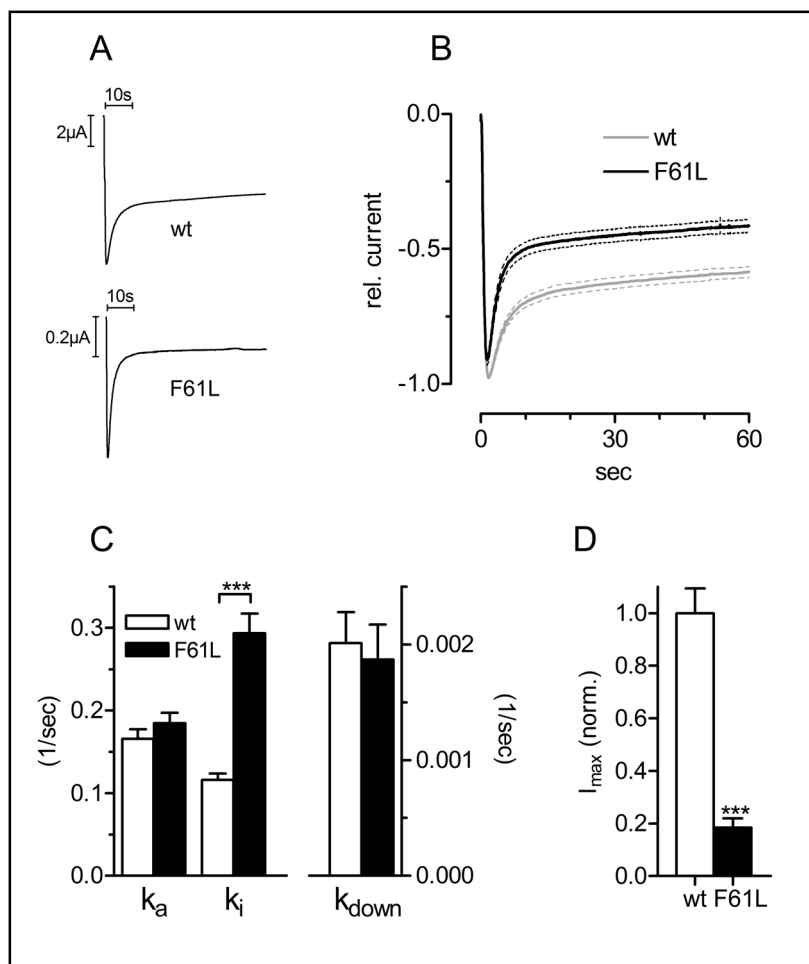
Recently, Lu et al. [30] reported that the specific small molecule ENaC-activator S3969 is able to rescue the reduced function of $\alpha\beta_{G37S}\gamma$ -ENaC, an ENaC mutant

which is known to cause PHA1 [41]. Since the α F61L mutation reduces ENaC function, we tested whether S3969 also rescues $\alpha_{F61L}\beta\gamma$ -ENaC. Fig. 6A shows two representative whole-cell current traces from an oocyte expressing $\alpha\beta\gamma$ -ENaC (left) or $\alpha_{F61L}\beta\gamma$ -ENaC (right). Application of S3969 (10 μ M) activated inward currents in both, $\alpha\beta\gamma$ -ENaC and $\alpha_{F61L}\beta\gamma$ -ENaC expressing oocytes. Results from similar experiments are summarized in Fig. 6B and confirm that the baseline ENaC currents measured before the application of S3969 were smaller in $\alpha_{F61L}\beta\gamma$ -ENaC than in $\alpha\beta\gamma$ -ENaC expressing oocytes. On average, S3969 increased ΔI_{ami} 2.2-fold in control oocytes and 4.7-fold in oocytes expressing $\alpha_{F61L}\beta\gamma$ -ENaC (Fig. 6C). In conclusion, our results demonstrate that S3969 can at least partially rescue the function of $\alpha_{F61L}\beta\gamma$ -ENaC.

Na⁺ self inhibition is enhanced in $\alpha_{F61L}\beta\gamma$ -ENaC

The so-called Na⁺ self inhibition is an inhibitory mechanism that inhibits ENaC within seconds when the extracellular Na⁺ concentration is acutely increased [31]. We wondered whether the α F61L mutation affects Na⁺ self inhibition. To test this we clamped $\alpha\beta\gamma$ -ENaC and $\alpha_{F61L}\beta\gamma$ -ENaC expressing oocytes at a holding potential of -100 mV and initially superfused the oocytes with a

Fig. 7. The α F61L mutation enhances Na^+ self inhibition of ENaC. A: Representative whole-cell current traces of an $\alpha\beta\gamma$ -ENaC (wt) and an $\alpha_{\text{F61L}}\beta\gamma$ -ENaC (F61L) expressing oocyte clamped at -100 mV. The traces show the whole-cell current response elicited by switching from a 1 mM to a 110 mM Na^+ bath solution. B: Normalized mean whole-cell current traces of wild-type ($n=22$, grey line) and mutant ENaC ($n=24$, black line) expressing oocytes from similar experiments as shown in A. Solid lines represent mean, dotted lines SE. C, D: Kinetic parameters (k_a , k_i , k_{down} , I_{max}) of the oocytes summarized in B derived from equation (1) as described in the methods. *** $p<0.001$



1 mM Na^+ containing bath solution. The representative whole-cell current trace shown in Fig. 7A (upper trace) demonstrates that in $\alpha\beta\gamma$ -ENaC expressing oocytes changing the bath solution from 1 mM Na^+ to 110 mM Na^+ resulted in a transient inward current peak. The rapid current decay after the peak increase represents Na^+ self inhibition [31]. Interestingly, we found that in $\alpha_{\text{F61L}}\beta\gamma$ -ENaC expressing oocytes this Na^+ self inhibition is even more pronounced (Fig. 7A, lower trace). Fig. 7B summarizes results from similar experiments by showing normalized average whole-cell current traces from wild-type $\alpha\beta\gamma$ -ENaC ($n=23$) and from $\alpha_{\text{F61L}}\beta\gamma$ -ENaC ($n=24$) expressing oocytes. The individual traces were fitted according to the model described by Chraïbi and Horisberger [31]. The activation rate constant k_a (wt: 0.17 ± 0.01 s $^{-1}$, α F61L: 0.18 ± 0.01 s $^{-1}$) and the rundown rate constant k_{down} (wt: 0.0020 ± 0.0003 s $^{-1}$, α F61L: 0.0018 ± 0.0003 s $^{-1}$) did not differ significantly between wt and mutant ENaC (Fig. 7C). However, the inactivation rate constant k_i was more than doubled in $\alpha_{\text{F61L}}\beta\gamma$ -ENaC (wt: 0.12 ± 0.01 s $^{-1}$, α F61L: 0.29 ± 0.02 s $^{-1}$, $p<0.001$). To correct for the batch to batch variability of ENaC

expression, individual I_{max} values were normalized to the mean I_{max} value measured for wild-type ENaC in the corresponding batch of oocytes. In $\alpha_{\text{F61L}}\beta\gamma$ -ENaC expressing oocytes I_{max} was about 80% lower than in $\alpha\beta\gamma$ -ENaC expressing oocytes (Fig. 7D). Taken together our findings indicate that an enhanced Na^+ self inhibition contributes to the reduced P_o of the mutant channel but is not its major cause.

Discussion

In the present study we compared the function of mutant $\alpha_{\text{F61L}}\beta\gamma$ -ENaC with wild-type $\alpha\beta\gamma$ -ENaC in the *Xenopus laevis* oocyte expression system. We found that the α F61L mutation reduced ENaC mediated whole-cell currents by about 90%. To rule out the possibility that this is an artifact arising from differences in oocyte or cRNA quality, we confirmed this finding in several different batches of oocytes with different batches of cRNAs. Moreover, in each experiment the injected cRNAs coding for the individual subunits including the

wild-type and mutant α -subunit were from cRNA batches synthesized in parallel to minimize the risk of variability in the cRNA quality. Thus, we are confident that the observed loss-of-function phenotype of the mutant channel is real. This is further supported by the fact that our present study confirms our recently reported preliminary data on this ENaC mutant [21].

In additional experiments we explored the underlying mechanism of the loss-of-function phenotype of the mutant channel. We investigated the surface expression of the channel using a chemiluminescence assay. These experiments revealed a $\sim 40\%$ decrease in channel density at the plasma membrane in oocytes expressing the mutant channel compared to oocytes expressing wild-type ENaC. The lower channel surface expression could result from a reduced overall protein expression of the mutant channel. However, we did not find any evidence for this in Western blot experiments (data not shown). Nevertheless, given the semi-quantitative nature of Western blot experiments, we cannot rule out a minor effect of the mutation on overall channel protein expression which may contribute to the reduced surface expression of the mutant channel. An alternative explanation for the reduced surface expression may be an altered trafficking of the mutant channel, i.e. reduced delivery of preformed channels to the plasma membrane, enhanced channel retrieval from the plasma membrane, or a combination of both effects. In the present study we did not further investigate the mechanism by which the mutation reduces channel surface expression, since the observed minor reduction cannot explain the pronounced loss-of-function phenotype of the mutant channel. Similarly, our single-channel recordings ruled out the possibility that a reduction of the single-channel conductance contributes to the loss-of-function phenotype of the mutant channel. Indeed, in our outside-out patch clamp experiments the single-channel conductance of the mutant channel was essentially identical to that of wild-type ENaC and averaged about 5 pS. This single-channel conductance value is consistent with data previously reported in the literature for human ENaC [33]. Thus, from our surface expression data and from our single-channel experiments we can conclude that the inhibitory effect of the mutation on the whole-cell ENaC currents must be caused mainly by a reduced activity of the channels present in the membrane, i.e. by a reduced average channel P_o .

To confirm this finding, we used the S520C mutation of human β ENaC as a tool to generate channels in which P_o can be increased experimentally. The β S520C mutation

is analogous to the previously described S518C mutation in the β -subunit of rat ENaC. Single-channel recordings of the latter have shown that this mutant channel can be converted to a channel with a P_o of close to one by application of the sulfhydryl reagent MTSET [25, 34]. The corresponding S520C mutation in human β ENaC behaves in a similar way [30, 35]. We demonstrated that the relative stimulatory effect of MTSET was about 4-fold larger on ENaC currents in oocytes expressing $\alpha_{F61L}\beta_{520C}\gamma$ -ENaC than in oocytes expressing $\alpha\beta_{520C}\gamma$ -ENaC. Since MTSET is thought to increase the P_o of ENaC from a given baseline value to nearly one, the MTSET effect is expected to be larger in a channel with a low baseline P_o . Thus, this finding supports our conclusion that the α F61L mutation reduces average baseline P_o of ENaC. Under the assumption that MTSET converted the P_o of all active ion channels present at the cell surface to one, we can estimate that in the oocyte system the average baseline P_o of the α F61L mutant channel is ~ 0.12 compared to an average baseline P_o of ~ 0.45 of the wild-type channel. This indicates that the α F61L mutation reduces the average baseline P_o of ENaC by about 75%. This estimated reduction of average baseline P_o in combination with the $\sim 40\%$ reduction of cell surface expression nicely explains the $\sim 90\%$ overall reduction of ENaC currents in the oocytes expressing mutant $\alpha_{F61L}\beta\gamma$ -ENaC.

In a second approach we tested the hypothesis that proteolytic channel activation by chymotrypsin is more pronounced in the α F61L mutant channel than in wild-type ENaC. Recent evidence indicates that proteolytic processing of ENaC along its biosynthetic pathway and at the cell surface is an important mechanism that contributes to ENaC activation in a complex manner [39]. Electrophysiological studies in the *Xenopus laevis* oocyte expression system have previously demonstrated a large and rapid stimulatory effect of extracellularly applied trypsin and chymotrypsin on ENaC activity [25, 36]. At present the precise molecular mechanism of proteolytic channel activation remains unclear. Cleavage occurs at specific sites within the extracellular loops of the α - and γ -subunits but not the β -subunit [38, 39, 42] and probably results in the release of inhibitory peptides from the extracellular loops of α - and γ ENaC [43-45]. In particular, cleavage of the γ -subunit appears to play a pivotal role in proteolytic ENaC activation [25, 46]. Proteolytic cleavage is thought to cause a conformational change of the channel favouring its open state which results in an increase in channel P_o . Thus, the relative stimulatory effect of an extracellular protease is likely to

be more pronounced on channels with a low baseline P_o than on highly active channels. Indeed, the relative stimulatory effect of chymotrypsin on the α F61L mutant channel was about 4-fold larger than that on wild-type ENaC. This supports our conclusion that the average baseline P_o of the α F61L mutant channel is much lower than that of wild-type ENaC.

Our whole-cell current measurements represent measurements of ensemble currents of many individual ion channels. Thus, from these measurements we can only estimate changes in average channel P_o . However, there is good evidence that at least two functionally distinct ENaC populations are present in the plasma membrane: Active channels with a somewhat variable but rather high P_o of about 0.5 [2] and near-silent channels with an exceedingly low P_o of less than 0.05 [1, 22, 47]. Extracellularly applied proteases appear to have a dual effect on ENaC open probability, activating near-silent channels [48, 49] and stimulating the gating of channels that are already active in the membrane [25]. Thus, the net effect is an overall increase in average P_o . It has been reported that ENaC with the β S520C subunit can be activated by MTSET only when the channel is in its open state [34]. Therefore, channels with long openings will be more readily activated than near-silent channels with very short openings. However, since the effect of MTSET was very similar to that of chymotrypsin, we can conclude that near-silent channels, at least occasionally, open long enough for MTSET to act on them and to convert them to channels with a high open probability. Thus, both MTSET and chymotrypsin are likely to increase the P_o of both, active and near-silent channels. The overall effect is an increase in average channel P_o reflected by an increase in ENaC whole-cell currents. Since the stimulatory effects of MTSET and of chymotrypsin were more pronounced in oocytes expressing the mutant α F61L channel, we have to assume that the average baseline P_o of the mutant channel is lower than that of the wild-type channel. Quantitatively the MTSET and chymotrypsin data are in good agreement and support our conclusion that the α F61L mutation reduces the average baseline P_o of ENaC by about 75 %.

In an additional set of experiments we explored the possibility that Na^+ self inhibition is enhanced in the mutant channel and may contribute to its reduced P_o . Na^+ self inhibition is a biophysical hallmark of ENaC and is a mechanism to prevent an intracellular Na^+ overload in transporting epithelial cells in the presence of a high extracellular Na^+ concentration [2, 34, 50-52].

The inhibitory effect of extracellular Na^+ on ENaC is rapid and caused by an acute decrease in channel P_o (Na^+ self inhibition) [31]. To investigate Na^+ self inhibition we used an established experimental protocol and calculated kinetic parameters according to a model described by Chraïbi and Horisberger [31]. Using this approach we could demonstrate that the inactivation rate constant k_p , which reflects the speed of Na^+ self inhibition, was more than doubled in the α F61L mutant channel. Thus, Na^+ self inhibition is indeed enhanced in the mutant channel. However, the mutation also reduced I_{max} , which represents the maximum current without the inhibitory effect of extracellular Na^+ , by about 80%. In comparison, under normal experimental conditions, when Na^+ self inhibition is active, the mutation reduced ENaC currents by about 90%. Thus, we can estimate that the enhanced Na^+ self inhibition contributes only about 10 % to the inhibitory effect of the α F61L mutation and cannot account for the ~75% reduction of P_o observed in the mutant channel.

At present we do not know by which molecular mechanism the α F61L mutation affects channel gating to reduce the P_o of ENaC. The mutation is localized in the N-terminal cytosolic region of the α -subunit. Interestingly, the N-terminus of the α -subunit has previously been reported to be involved in the modulation of channel gating [53]. This was concluded from the observation that substitution of H94, G95, or R98 in rat α ENaC (corresponding to H69, G70, or R73 in human α ENaC) by alanine reduced ENaC currents and surface expression to a similar degree as observed in the present study for α F61L. However, when the residue corresponding to human α F61 in rat, F86, was substituted by alanine, no effect on ENaC currents was observed [53]. This may be attributed to the fact that alanine rather than leucine was used to substitute the phenylalanine residue. An alternative explanation is a species difference. In fact, despite the high similarity of the human and rat amino acid sequence in this region, the amino acid directly preceding the critical α F61/F86 residue differs in charge with E60 in human and Q85 in rat. Nevertheless, our findings tend to support the general conclusion that the N-terminal cytosolic region of α ENaC is likely to contain amino acid residues that are critical for channel gating.

Pharmacological restoration of impaired channel function would be an intriguing therapeutic tool in diseases caused by ENaC loss-of-function mutations. Recently, it has been shown that an ENaC activator called S3969 can largely restore the function of a mutant ENaC with the β G37S loss-of-function mutation [30] identified in

PHA1 patients [14]. We could demonstrate that S3969 can also activate ENaC with the α F61L mutation. In the presence of the S3969 activator, ENaC currents of oocytes expressing the α F61L channel reached similar levels as observed in oocytes expressing wild-type ENaC under baseline conditions in the absence of S3969. This result suggests that in principle it should be possible to treat symptoms caused by the α F61L mutations by using a specific ENaC activator. Moreover, in patients suffering from respiratory symptoms as a result of ENaC loss-of-function mutations, specific activators of ENaC may reach their target in the apical membrane of airway epithelial cells by inhalation therapy which would reduce the risk of systemic side effects of the activator.

In summary we have shown that the α F61L mutation identified in a patient diagnosed with atypical CF mediates an inhibitory effect on ENaC which is mainly caused by a reduction of channel P_o and, to a lesser extent, by a reduction of channel surface expression. In addition, we could demonstrate that the ENaC activator S3969 can largely restore the function of the mutant channel. Since loss-of-function mutations of ENaC in patients with PHA1 have been reported to be associated with CF-like pulmonary symptoms, it is tempting to speculate that the α F61L mutation contributes to the pulmonary symptoms of patients carrying

this mutation. At present it is unclear why some loss-of-function mutations of ENaC mainly manifest as a renal salt wasting syndrome (PHA1) while others cause CF-like pulmonary symptoms without overt renal disease. Organ specific differences in ENaC processing and activation and differences in the genetic background may be responsible for the development of different disease phenotypes.

Acknowledgements

We acknowledge the expert technical assistance of Ralf Rinke, Sonja Mayer, Jessica Ott and Céline Harlay. This study was supported by grants from the Johannes and Frieda Marohn-Stiftung at the University Erlangen-Nürnberg, from the Interdisziplinäres Zentrum für Klinische Forschung (IZKF) of the Medical Faculty of the University of Erlangen-Nürnberg, from the Deutsche Forschungsgemeinschaft (DFG, SFB423: Kidney injury: Pathogenesis and Regenerative Mechanism), from the Alphonse and Jean Forton Fund - Koning Boudewijn Stichting (2005 04 R7 115 BO and 2008-R10150-002), and from the Het Fonds voor Wetenschappelijk Onderzoek Vlaanderen (G.0521.06 and 1.5.111.07).

References

- 1 Kellenberger S, Schild L: Epithelial sodium channel/degenerin family of ion channels: a variety of functions for a shared structure. *Physiol Rev* 2002;82:735-767.
- 2 Garty H, Palmer LG: Epithelial sodium channels: function, structure, and regulation. *Physiol Rev* 1997;77:359-396.
- 3 Hummler E, Barker P, Gatzky J, Beermann F, Verdumo C, Schmidt A, Boucher R, Rossier BC: Early death due to defective neonatal lung liquid clearance in alpha-ENaC-deficient mice. *Nat Genet* 1996;12:325-328.
- 4 Canessa CM: Structural biology: unexpected opening. *Nature* 2007;449:293-294.
- 5 Jasti J, Furukawa H, Gonzales EB, Gouaux E: Structure of acid-sensing ion channel 1 at 1.9 Å resolution and low pH. *Nature* 2007;449:316-323.
- 6 Stockand JD, Staruschenko A, Pochynyuk O, Booth RE, Silverthorn DU: Insight toward epithelial Na⁺ channel mechanism revealed by the acid-sensing ion channel 1 structure. *IUBMB Life* 2008;60:620-628.
- 7 De Boeck K, Wilschanski M, Castellani C, Taylor C, Cuppens H, Dodge J, Sinaasappel M: Cystic fibrosis: terminology and diagnostic algorithms. *Thorax* 2006;61:627-635.
- 8 Stanke F, Becker T, Cuppens H, Kumar V, Cassiman JJ, Jansen S, Radojkovic D, Siebert B, Yarden J, Ussery DW, Wienker TF, Tummler B: The TNFa receptor TNFRSF1A and genes encoding the amiloride-sensitive sodium channel ENaC as modulators in cystic fibrosis. *Hum Genet* 2006;119:331-343.

- 9 Boucher RC: New concepts of the pathogenesis of cystic fibrosis lung disease. *Eur Respir J* 2004;23:146-158.
- 10 Grubb BR, Boucher RC: Pathophysiology of gene-targeted mouse models for cystic fibrosis. *Physiol Rev* 1999;79:S193-214.
- 11 Snouwaert JN, Brigman KK, Latour AM, Malouf NN, Boucher RC, Smithies O, Koller BH: An animal model for cystic fibrosis made by gene targeting. *Science* 1992;257:1083-1088.
- 12 Mall M, Grubb BR, Harkema JR, O'Neal WK, Boucher RC: Increased airway epithelial Na⁺ absorption produces cystic fibrosis-like lung disease in mice. *Nat Med* 2004;10:487-493.
- 13 Zhou Z, Treis D, Schubert SC, Harm M, Schattner J, Hirtz S, Duerr J, Boucher RC, Mall MA: Preventive but not late amiloride therapy reduces morbidity and mortality of lung disease in bENaC-overexpressing mice. *Am J Respir Crit Care Med* 2008;178:1245-1256.
- 14 Chang SS, Grunder S, Hanukoglu A, Rosler A, Mathew PM, Hanukoglu I, Schild L, Lu Y, Shimkets RA, Nelson-Williams C, Rossier BC, Lifton RP: Mutations in subunits of the epithelial sodium channel cause salt wasting with hyperkalaemic acidosis, pseudohypaldosteronism type 1. *Nat Genet* 1996;12:248-253.
- 15 Hanukoglu A, Bistrizter T, Rakover Y, Mandelberg A: Pseudohypaldosteronism with increased sweat and saliva electrolyte values and frequent lower respiratory tract infections mimicking cystic fibrosis. *J Pediatr* 1994;125:752-755.
- 16 Marthinsen L, Kornfalt R, Aili M, Andersson D, Westgren U, Schaedel C: Recurrent *Pseudomonas* bronchopneumonia and other symptoms as in cystic fibrosis in a child with type I pseudohypaldosteronism. *Acta Paediatr* 1998;87:472-474.
- 17 Schaedel C, Marthinsen L, Kristofferson AC, Kornfalt R, Nilsson KO, Orlenius B, Holmberg L: Lung symptoms in pseudohypaldosteronism type 1 are associated with deficiency of the alpha-subunit of the epithelial sodium channel. *J Pediatr* 1999;135:739-745.
- 18 Sheridan MB, Fong P, Groman JD, Conrad C, Flume P, Diaz R, Harris C, Knowles M, Cutting GR: Mutations in the beta-subunit of the epithelial Na⁺ channel in patients with a cystic fibrosis-like syndrome. *Hum Mol Genet* 2005;14:3493-3498.
- 19 Kerem E, Bistrizter T, Hanukoglu A, Hofmann T, Zhou Z, Bennett W, MacLaughlin E, Barker P, Nash M, Quittell L, Boucher R, Knowles MR: Pulmonary epithelial sodium-channel dysfunction and excess airway liquid in pseudohypaldosteronism. *N Engl J Med* 1999;341:156-162.
- 20 Cutting GR: Genetic heterogeneity and cystic fibrosis. *Hum Mutat* 2009;30:v.
- 21 Azad AK, Rauh R, Vermeulen F, Jaspers M, Korbmacher J, Boissier B, Bassinet L, Fichou Y, Georges MD, Stanke F, De Boeck K, Dupont L, Balascakova M, Hjelte L, Lebecque P, Radojkovic D, Castellani C, Schwartz M, Stuhmann M, Schwarz M, Skalicka V, de Monestrol I, Girodon E, Ferec C, Claustres M, Tummler B, Cassiman JJ, Korbmacher C, Cuppens H: Mutations in the amiloride-sensitive epithelial sodium channel in patients with cystic fibrosis-like disease. *Hum Mutat* 2009;30:1093-1103.
- 22 Firsov D, Schild L, Gautschi I, Merillat AM, Schneeberger E, Rossier BC: Cell surface expression of the epithelial Na channel and a mutant causing Liddle syndrome: a quantitative approach. *Proc Natl Acad Sci U S A* 1996;93:15370-15375.
- 23 Wielputz MO, Lee IH, Dinudom A, Boukroun S, Farman N, Cook DI, Korbmacher C, Rauh R: NDRG2 Stimulates Amiloride-sensitive Na⁺ Currents in *Xenopus laevis* Oocytes and Fisher Rat Thyroid Cells. *J Biol Chem* 2007;282:28264-28273.
- 24 Rauh R, Dinudom A, Fotia AB, Paulides M, Kumar S, Korbmacher C, Cook DI: Stimulation of the epithelial sodium channel (ENaC) by the serum- and glucocorticoid-inducible kinase (Sgk) involves the PY motifs of the channel but is independent of sodium feedback inhibition. *Pflugers Arch* 2006;452:290-299.
- 25 Diakov A, Bera K, Mokrushina M, Krueger B, Korbmacher C: Cleavage in the g-subunit of the epithelial sodium channel (ENaC) plays an important role in the proteolytic activation of near-silent channels. *J Physiol* 2008;586:4587-4608.
- 26 Diakov A, Korbmacher C: A novel pathway of epithelial sodium channel activation involves a serum- and glucocorticoid-inducible kinase consensus motif in the C terminus of the channel's alpha-subunit. *J Biol Chem* 2004;279:38134-38142.
- 27 Korbmacher C, Volk T, Segal AS, Boulpaep EL, Fromter E: A calcium-activated and nucleotide-sensitive nonselective cation channel in M-1 mouse cortical collecting duct cells. *J Membr Biol* 1995;146:29-45.
- 28 Zerangue N, Schwappach B, Jan YN, Jan LY: A new ER trafficking signal regulates the subunit stoichiometry of plasma membrane K(ATP) channels. *Neuron* 1999;22:537-548.
- 29 Konstas AA, Bielfeld-Ackermann A, Korbmacher C: Sulfonylurea receptors inhibit the epithelial sodium channel (ENaC) by reducing surface expression. *Pflugers Arch* 2001;442:752-761.
- 30 Lu M, Echeverri F, Kalabat D, Laita B, Dahan DS, Smith RD, Xu H, Staszewski L, Yamamoto J, Ling J, Hwang N, Kimmich R, Li P, Patron E, Keung W, Patron A, Moyer BD: Small molecule activator of the human epithelial sodium channel. *J Biol Chem* 2008;283:11981-11994.
- 31 Chraibi A, Horisberger JD: Na self inhibition of human epithelial Na channel: temperature dependence and effect of extracellular proteases. *J Gen Physiol* 2002;120:133-145.
- 32 Kellenberger S, Gautschi I, Rossier BC, Schild L: Mutations causing Liddle syndrome reduce sodium-dependent downregulation of the epithelial sodium channel in the *Xenopus* oocyte expression system. *J Clin Invest* 1998;101:2741-2750.
- 33 Waldmann R, Champigny G, Bassilana F, Voilley N, Lazdunski M: Molecular cloning and functional expression of a novel amiloride-sensitive Na⁺ channel. *J Biol Chem* 1995;270:27411-27414.
- 34 Kellenberger S, Gautschi I, Schild L: An external site controls closing of the epithelial Na⁺ channel ENaC. *J Physiol* 2002;543:413-424.
- 35 Snyder PM, Bucher DB, Olson DR: Gating induces a conformational change in the outer vestibule of ENaC. *J Gen Physiol* 2000;116:781-790.
- 36 Chraibi A, Vallet V, Firsov D, Hess SK, Horisberger JD: Protease modulation of the activity of the epithelial sodium channel expressed in *Xenopus* oocytes. *J Gen Physiol* 1998;111:127-138.
- 37 Kleyman TR, Myerburg MM, Hughey RP: Regulation of ENaCs by proteases: An increasingly complex story. *Kidney Int* 2006;70:1391-1392.
- 38 Kleyman TR, Carattino MD, Hughey RP: ENaC at the cutting edge: regulation of epithelial sodium channels by proteases. *J Biol Chem*. 2009;284:20447-51.
- 39 Rossier BC, Stutts MJ: Activation of the epithelial sodium channel (ENaC) by serine proteases. *Annu Rev Physiol* 2009;71:361-379.
- 40 Durieux ME, Salafranca MN, Lynch KR: Trypsin induces Ca²⁺-activated Cl⁻ currents in *X. laevis* oocytes. *FEBS Lett* 1994;337:235-238.
- 41 Grunder S, Firsov D, Chang SS, Jaeger NF, Gautschi I, Schild L, Lifton RP, Rossier BC: A mutation causing pseudohypaldosteronism type 1 identifies a conserved glycine that is involved in the gating of the epithelial sodium channel. *EMBO J* 1997;16:899-907.

- 42 Planes C, Caughey GH: Regulation of the epithelial Na⁺ channel by peptidases. *Curr Top Dev Biol* 2007;78:23-46.
- 43 Bruns JB, Carattino MD, Sheng S, Maarouf AB, Weisz OA, Pilewski JM, Hughey RP, Kleyman TR: Epithelial Na⁺ channels are fully activated by furin- and prostaticin-dependent release of an inhibitory peptide from the gamma-subunit. *J Biol Chem* 2007;282:6153-6160.
- 44 Carattino MD, Passero CJ, Steren CA, Maarouf AB, Pilewski JM, Myerburg MM, Hughey RP, Kleyman TR: Defining an inhibitory domain in the alpha-subunit of the epithelial sodium channel. *Am J Physiol Renal Physiol* 2008;294:F47-52.
- 45 Carattino MD, Sheng S, Bruns JB, Pilewski JM, Hughey RP, Kleyman TR: The epithelial Na⁺ channel is inhibited by a peptide derived from proteolytic processing of its alpha subunit. *J Biol Chem* 2006;281:18901-18907.
- 46 Carattino MD, Hughey RP, Kleyman TR: Proteolytic processing of the epithelial sodium channel gamma subunit has a dominant role in channel activation. *J Biol Chem* 2008;283:25290-25295.
- 47 Rossier BC: Hormonal regulation of the epithelial sodium channel ENaC: N or P(o)? *J Gen Physiol* 2002;120:67-70.
- 48 Caldwell RA, Boucher RC, Stutts MJ: Serine protease activation of near-silent epithelial Na⁺ channels. *Am J Physiol Cell Physiol* 2004;286:C190-194.
- 49 Caldwell RA, Boucher RC, Stutts MJ: Neutrophil elastase activates near-silent epithelial Na⁺ channels and increases airway epithelial Na⁺ transport. *Am J Physiol Lung Cell Mol Physiol* 2005;288:L813-819.
- 50 Bize V, Horisberger JD: Sodium self-inhibition of human epithelial sodium channel: selectivity and affinity of the extracellular sodium sensing site. *Am J Physiol Renal Physiol* 2007;293:F1137-1146.
- 51 Horisberger JD, Chraïbi A: Epithelial sodium channel: a ligand-gated channel? *Nephron Physiol* 2004;96:p37-41.
- 52 Turnheim K: Intrinsic regulation of apical sodium entry in epithelia. *Physiol Rev* 1991;71:429-445.
- 53 Grunder S, Jaeger NF, Gautschi I, Schild L, Rossier BC: Identification of a highly conserved sequence at the N-terminus of the epithelial Na⁺ channel alpha subunit involved in gating. *Pflugers Arch* 1999;438:709-715.